A MODIFIED PLASTIC THEORY OF REINFORCED CONCRETE

PAUL ANDERSEN, Ph.D.
Professor of Structural Engineering

HWA-NI LEE, Ph.D.
Formerly Instructor, Department
of Mathematic and Mechanics

BULLETIN NO. 33

UNIVERSITY OF MINNESOTA
J. L. MORRILL, President
INSTITUTE OF TECHNOLOGY
A. F. SPILHAUS, Dean
ENGINEERING EXPERIMENT STATION
R. E. MONTONNA, Director

VOL. LIV NO. 19 APRIL 16, 1951

Entered at the post office in Minneapolis as semi-monthly second-class matter, Minneapolis, Minnesota. Accepted for mailing at special rate of postage provided for in Section 1103, Act of October 3, 1917, authorized July 12, 1918.

ACKNOWLEDGMENT

The investigations and tests described in this bulletin were conducted as a research problem in the Engineering Experiment Station of the University of Minnesota.

The test specimens, together with their steel end brackets, were designed by the senior author and used previously for testing reinforced concrete sections subjected to eccentric loads. The actual work of loading and recording, as well as the greater part of the theoretical investigation, was done by the junior author as a portion of his thesis for the degree of Doctor of Philosophy.

The authors gratefully acknowledge the help and encouragement given by Dr. Ralph E. Montonna and Professor C. E. Lund of the Engineering Experiment Station of the University of Minnesota.

TABLE OF CONTENTS

ILLUSTRATIONS

TABLES

INTRODUCTION

The plastic theories of concrete are based on a phenomenon which has been early recognized. In 1906, Arthur Newell Talbot[1] stated:

> "Various curves have been proposed to represent the stress-deformation relation for concrete, but the parabola is the most satisfactory general representation. Frequently, the parabola expresses the relation almost exactly and in nearly every case the parabolic relation will fit the stress-deformation diagram very closely through the part which is ordinarily developed in beams. . . . Even if the straight line relation be accepted as sufficient for use with ordinary working stresses, the parabolic or other variable relation must be used in discussing experimental data when any considerable deformation is developed in the concrete."

Since this statement was made, more than 45 years ago, many attempts have been made to write formulas for reinforced concrete design based on a curved stress-deformation diagram, but most of the progress has been made during the past decade. The most notable contributions have been those of C. S. Whitney[2] and V. P. Jensen,[3] which for the sake of simplification substitute for the curved stress-deformation diagram a rectangle and trapezoid respectively.

In this bulletin are presented formulas for stresses in reinforced concrete based on a parabolic stress-deformation relationship. Additional assumptions made are those of preservation of plane sections and disregard of any tensile stresses which may exist in the concrete.

---

[1] University of Illinois, Engineering Experiment Station Bulletin No. 4, April, 1906.

[2] Transactions A. S. C. E., Vol. 107, 1942, p. 251.

[3] University of Illinois, Engineering Experiment Station Bulletin No. 345, June, 1943.

NOMENCLATURE

The following symbols are used:

A	coefficient of stress-strain curve of concrete
A_s	area of steel (tension, compression or total)
A'_s	area of additional steel in compression
B	coefficient of stress-strain curve of concrete
b	width of section
C	total compression in concrete
D	length of diagonal of square section
D'	distance center to center of the two steel bars on the diagonal of square section
d	distance from extreme fiber in compression to the center of gravity of steel in tension
d'	distance from extreme fiber in tension or compression to the center of gravity of the steel in tension or compression respectively
δ	deflection
δ_1	lateral deflection of column shaft
δ_2	lateral deflection of enlarged portion of test specimen
E_s	modulus of elasticity of steel
e	eccentricity
ϵ	unit strain of fiber at a distance x from the neutral axis
ϵ_s	average unit strain of steel fiber in compression or tension
f_c	intensity of fiber stress in concrete
f'_c	standard control cylinder strength of concrete
f_s	average intensity of fiber stress in steel in tension or compression
f_y	average intensity of fiber stress in steel in compression or tension at the yield point of steel
j	ratio of distance from the tension steel to the centroid of the compression forces to the depth
k	ratio of distance from extreme compression fiber to neutral axis to depth
l	length of column

l_1	length of center portion of test specimen
l_2	length of enlarged portion of test specimen
M	internal resisting moment
P	concentrated column load
p	ratio of cross-sectional area of steel to cross-sectional area of section
p_o	critical steel ratio
T	total tension in steel
t	total depth of section
X	unit strain of fiber in compression at one unit distance from the neutral axis
x	distance from fiber to neutral axis
x_1	distance from neutral axis to centroid of compression volume
x_1'	distance from the center of the section to the centroid of compression volume

BENDING OF REINFORCED CONCRETE

Conventional analysis of reinforced concrete assumes a linear distribution of stress over sections subjected to the action of bending moments. This, it has long been recognized, is not in accordance with test results and leads to uneconomical dimensions and amounts of reinforcements. A parabolic stress distribution has been suggested by several writers and will be discussed in the following.

The theoretical considerations will be based on the assumptions that the plane sections before bending remain plane after bending, and that any tension resisted by the concrete can be disregarded. Instead of the conventional "Hooke's law," it will be assumed that the stress, f_c, varies with the strain, ϵ, according to a second degree parabola, thus

$$f_c = A\epsilon - B\epsilon^2 \qquad (1)$$

Figure 1 shows the stress-strain diagram for a concrete cylinder which was tested together with four others and to which reference will be made. Applying Equation (1) to the test results gives

$$f_c = 544 \times 10^4 \epsilon - 1359 \times 10^6 \epsilon^2$$

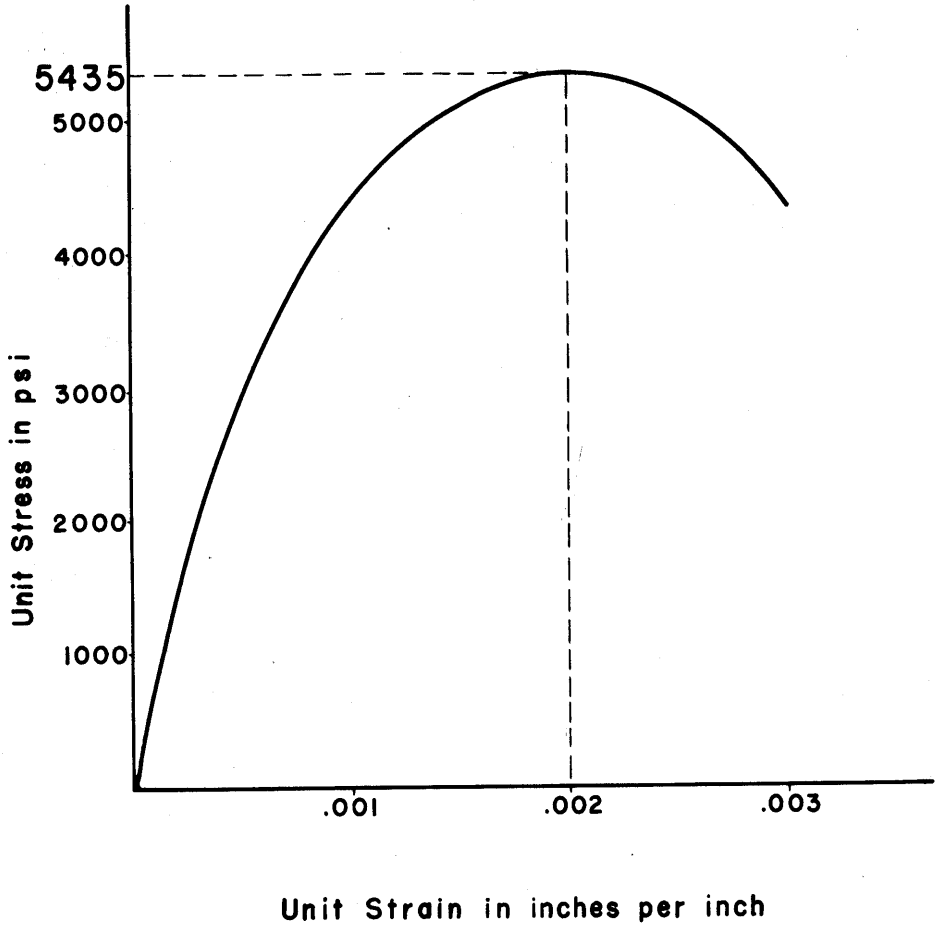

Figure 1

Stress-Strain Curve

In order to apply Equation (1) to a concrete beam reinforced for tension, it is assumed in Figure 2 that X is the strain at a unit distance from the neutral axis, then

$$\epsilon = Xx \qquad (2)$$

Equation (1) can be written

$$f_c = AXx - BX^2x^2 \qquad (3)$$

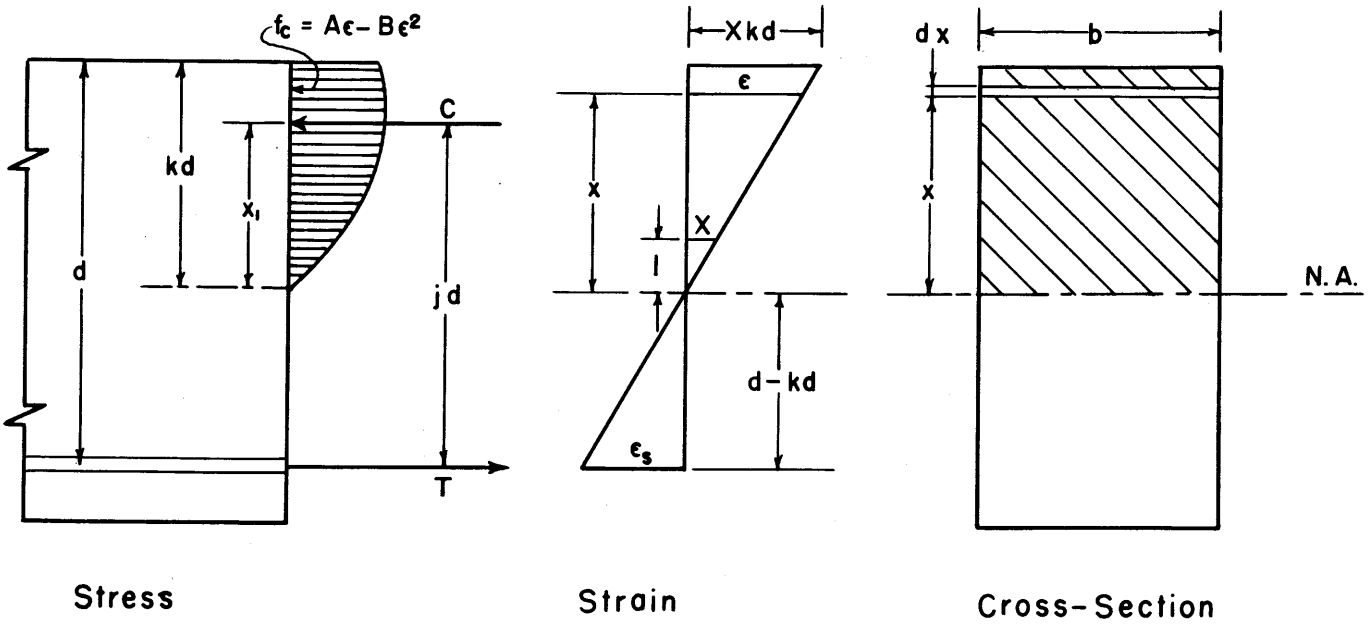

Figure 2

Rectangular Section in Bending

The total compression above the neutral axis will be

$$C = \int_0^{kd} f_c b\,dx = bXk^2d^2\left[\frac{A}{2} - \frac{BXkd}{3}\right] \qquad (4)$$

The position of this resultant force is found by taking moments about the neutral axis, thus

$$x_1 = \frac{1}{C}\int_0^{kd} x f_c b\,dx = kd\,\frac{4A - 3BXkd}{6A - 4BXkd} \qquad (5)$$

The elongation of the steel bars will be proportional to their distance from the neutral axis, thus

$$\epsilon_s = d(1-k)X \qquad (6)$$

and the total steel stress will equal

$$A_s f_s = E_s d(1-k)XA_s \qquad (7)$$

Equating Equations (4) and (7) and substituting $p = A_s \div bd$ give

$$k^2\left(\frac{A}{2} - \frac{BXkd}{3}\right) = pE_s(1-k) \qquad (8)$$

If the steel stress has reached the yield point, f_y, this equation will change to

$$Xk^2d\left(\frac{A}{2} - \frac{BXkd}{3}\right) = pf_y \qquad (8a)$$

The distance from the steel to the centroid of the compression forces will be

$$jd = d\left(1 - k\frac{2A - BXkd}{6A - 4BXkd}\right) \qquad (9)$$

The resisting moment of the beam section can be found by multiplication of Equations (4) and (9), thus

$$M = Cjd = bd^3k^2X\left[\frac{A}{6}(3-k) - \frac{B}{12}Xkd(4-k)\right] \qquad (10)$$

In order to find the quantity, X, which will give maximum bending moment, Equation (10) is differentiated with respect to X and the derivative placed equal to zero and solved for X, thus

$$\frac{\partial M}{\partial X} = 0 \; ; \; X = \frac{A(3-k)}{Bkd(4-k)} \qquad (11)$$

Substituting this value for X in Equation (10) gives

$$M = \frac{A^2}{B}\frac{k(3-k)}{12(4-k)}bd^2 \qquad (12)$$

If the beam is under-reinforced, primary failure will occur in the steel, and the location of the neutral axis can be found by eliminating X between Equations (8a) and (11), thus

$$\frac{k(3-k)(6-k)}{6(4-k)^2} = \frac{B}{A^2}f_y p \qquad (13)$$

Since the value of k is always less unity, an examination of the left side of Equation (13) shows that a very close approximation is 3/16k or

$$k = \frac{16}{3} f_y p \frac{B}{A^2} \qquad (14)$$

For the over-reinforced beam the steel stress at rupture will be less than the yield point. Elimination of X between Equations (8) and (11) gives

$$\frac{k^2(6-k)}{6(4-k)(1-k)} = \frac{pE_s}{A} \qquad (15)$$

In order to find the critical steel percentage (for which yield point stress will be reached before crushing failure of concrete), it is noted that a consequence of the preservation of plane sections is that the elongation ϵ_y of the tensile reinforcement will equal

$$\epsilon_y = d(1-k)X \qquad (16)$$

Substituting the value for X from Equation (11) and solving for k give

$$k = 2 - \sqrt{\frac{4\epsilon_y + (A \div B)}{\epsilon_y + (A \div B)}} \qquad (17)$$

If p_o is the critical steel percentage and Equations (14) and (17) are made equal, it is seen that

$$p_o = \frac{3}{16} \frac{A^2}{B f_y} \left[2 - \sqrt{\frac{4\epsilon_y + (A \div B)}{\epsilon_y + (A \div B)}} \right] \qquad (18)$$

AXIAL LOAD AND TRANSVERSE BENDING

Case I. Neutral Axis within Section

In a column section, as shown in Figure 3, the total compression in the concrete can be expressed thus

$$C = bXk^2t^2\left[\frac{A}{2} - \frac{BXkt}{3}\right] \qquad (4)$$

In order to find the quantity, X, which will give maximum axial load, this equation is differentiated with respect to X and the derivative placed equal to zero and solved for X thus

$$\frac{\partial C}{\partial X} = 0; \qquad X = \frac{3A}{4Bkt} \qquad (19)$$

Eliminating X between Equations (4) and (19)

$$C = \frac{3}{16}\frac{A^2kbt}{B} \qquad (20)$$

Substituting Equation (19) in Equation (5) gives the distance from the neutral axis to the centroid of the compression volume

$$x_1 = \frac{7}{12}kt \qquad (21)$$

Projecting all forces in Figure 3 on a vertical line gives

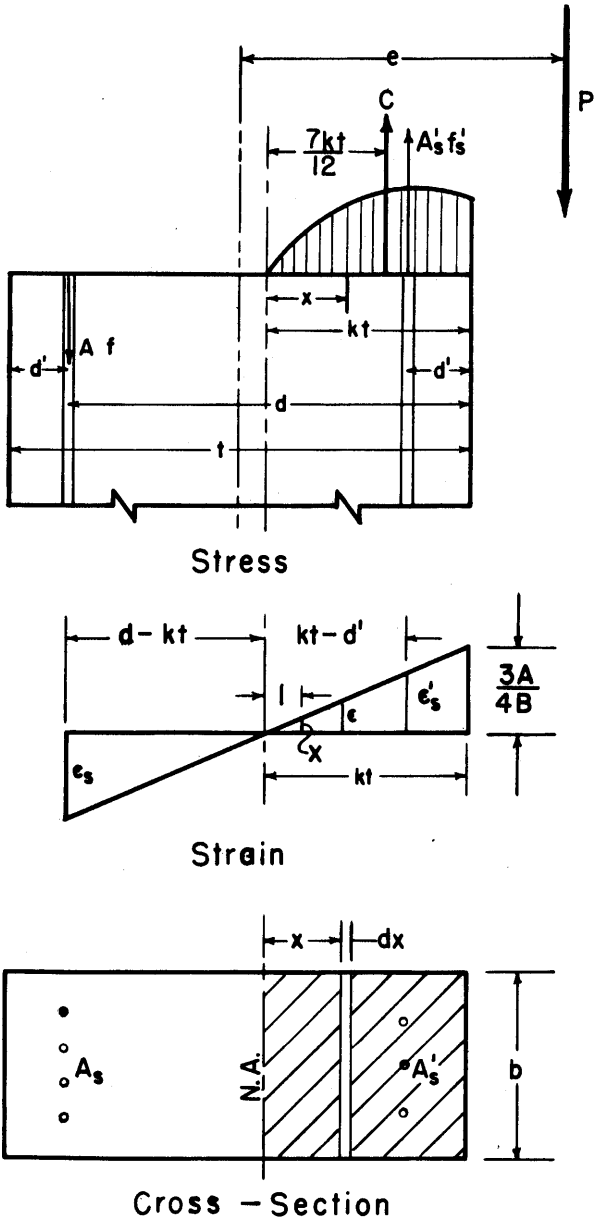

Figure 3

Axial Load and Transverse Bending, Case I

$$P = \frac{3}{16}\frac{A^2kbt}{B} + A'_s f'_s - A_s f_s \qquad (22)$$

Taking moments of all forces about the center line gives

$$Pe = \frac{3}{16}\frac{A^2kbt}{B} \times \frac{t}{2} \times \frac{6-5k}{6} + \left(\frac{t}{2} - d'\right)\left(A_s f_s + A'_s f'_s\right) \qquad (23)$$

Eliminating P between Equations (22) and (23) gives

$$k^2 + \frac{12}{5}\left(\frac{e}{t} - \frac{1}{2}\right)k + \frac{64}{5}\frac{B}{A^2}\left[\frac{A'_s f'_s}{bt}\left(\frac{e}{t} - \frac{1}{2} + \frac{d'}{t}\right)\right.$$

$$\left. - \frac{A_s f_s}{bt}\left(\frac{e}{t} + \frac{1}{2} - \frac{d'}{t}\right)\right] = 0 \qquad (24)$$

If the steel areas in the two flanges are equal, this equation becomes

$$k^2 + \frac{12}{5}\left(\frac{e}{t} - \frac{1}{2}\right)k + \frac{32}{5}\frac{B}{A^2}p\left[f'_s\left(\frac{e}{t} - \frac{1}{2} + \frac{d'}{t}\right)\right.$$

$$\left. - f_s\left(\frac{e}{t} + \frac{1}{2} - \frac{d'}{t}\right)\right] = 0 \qquad (25)$$

Examination of Figure 3 shows that

$$f'_s = \frac{3A}{4B}\left(1 - \frac{d'}{kt}\right)E_s$$

and

$$f_s = \frac{3A}{4B}\left(\frac{d}{kt} - 1\right)E_s$$

Case II. Neutral Axis Outside Section

In the case of compression over the entire section, it can be seen from Figure 4 that the total compression on the concrete will be

$$C = \int_{kt-t}^{kt} (AXx - BX^2x^2)b\,dx$$

or

$$C = bXt^2\left[A\left(k-\frac{1}{2}\right) - BXt\left(k^2-k+\frac{1}{3}\right)\right] \qquad (26)$$

Differentiating with respect to X and placing equal to zero give

$$\frac{\partial C}{\partial X} = 0; \qquad X = \frac{A\left(k-\frac{1}{2}\right)}{2Bt\left(k^2-k+\frac{1}{3}\right)} \qquad (27)$$

Substituting Equation (27) in Equation (26)

$$C = \frac{bt}{4}\frac{A^2}{B}\frac{k(k-1)+\frac{1}{4}}{k(k-1)+\frac{1}{3}} \qquad (28)$$

In order to facilitate numerical computations, the variation of the function

$$C(k) = \frac{k(k-1)+\frac{1}{4}}{4\left[k(k-1)+\frac{1}{3}\right]} \qquad (29)$$

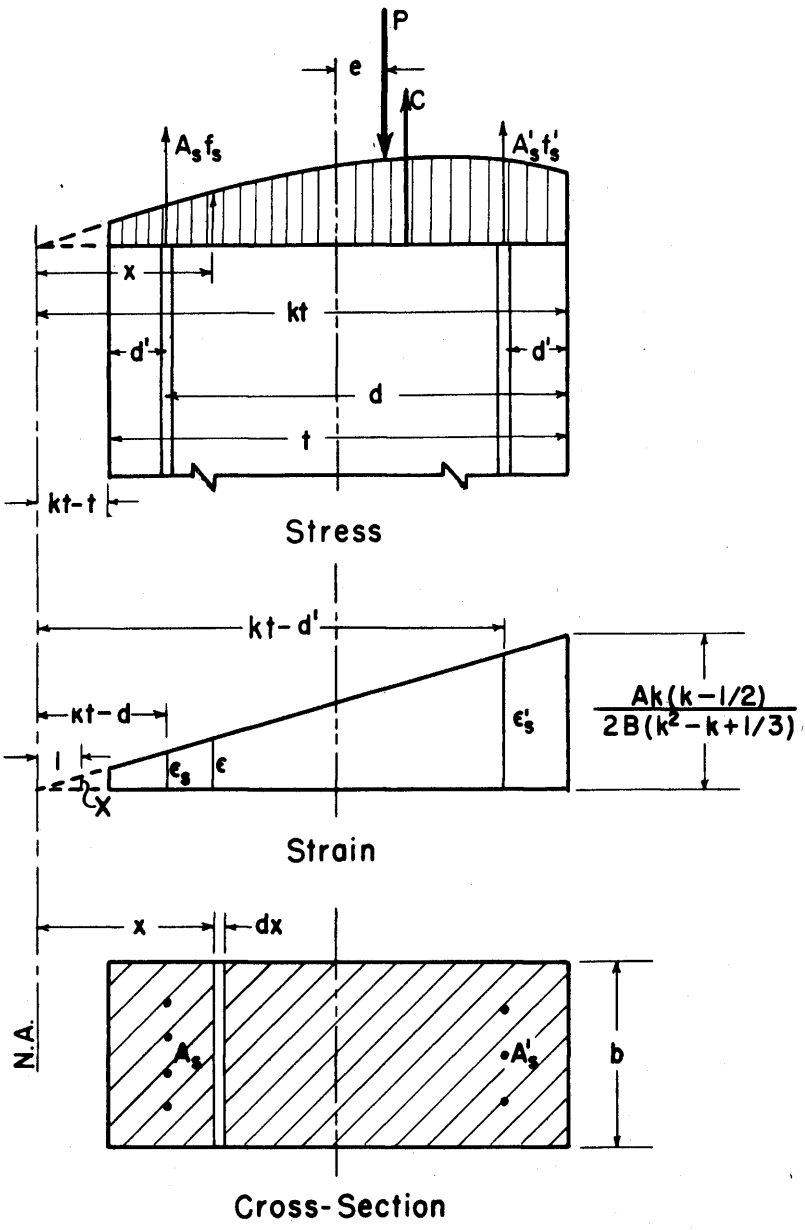

Figure 4

Axial Load and Transverse Bending, Case II

has been plotted in Figure 5. The distance from the neutral axis to the centroid of the stress volume can be found by taking static moments about the axis, thus

$$x_1 = \frac{\int f_c x dA}{C} = \frac{\int_{kt-t}^{kt} (A\epsilon - B\epsilon^2) x b dx}{\frac{bt}{4}\frac{A^2}{B}\frac{k(k-1)+\frac{1}{4}}{k(k-1)+\frac{1}{3}}} \qquad (30)$$

Substituting in this expression $\epsilon = Xx$ completing the integration and substituting Equation (27) give

$$x_1 = \frac{k^4 - 2k^3 + \frac{19}{12}k^2 - \frac{7}{12}k + \frac{7}{72}}{\left(k-\frac{1}{2}\right)\left(k^2-k+\frac{1}{3}\right)} t \qquad (31)$$

The distance from the center of the section to the centroid of the stress volume is seen from Figure 4 to equal

$$x_1' = \left[\frac{k^4 - 2k^3 + \frac{19}{12}k^2 - \frac{7}{12}k + \frac{7}{72}}{\left(k-\frac{1}{2}\right)\left(k^2-k+\frac{1}{3}\right)} - k + \frac{1}{2}\right] t \qquad (32)$$

In order to facilitate the numerical computations, the function

$$Z(k) = \frac{k^4 - 2k^3 + \frac{19}{12}k^2 - \frac{7}{12}k + \frac{7}{72}}{\left(k-\frac{1}{2}\right)\left(k^2-k+\frac{1}{3}\right)} - k + \frac{1}{2} \qquad (33)$$

has also been plotted in Figure 5. Projecting all forces on a vertical line gives

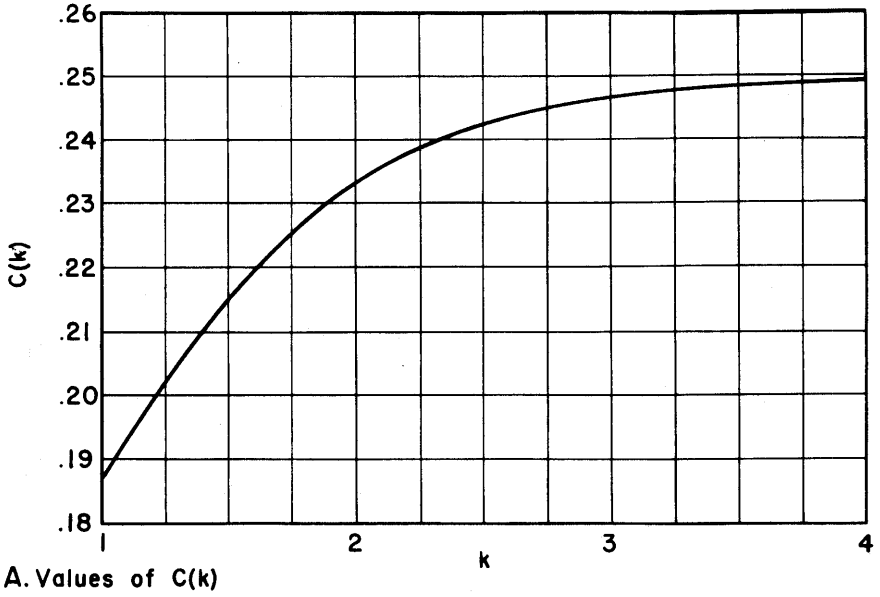

A. Values of C(k)

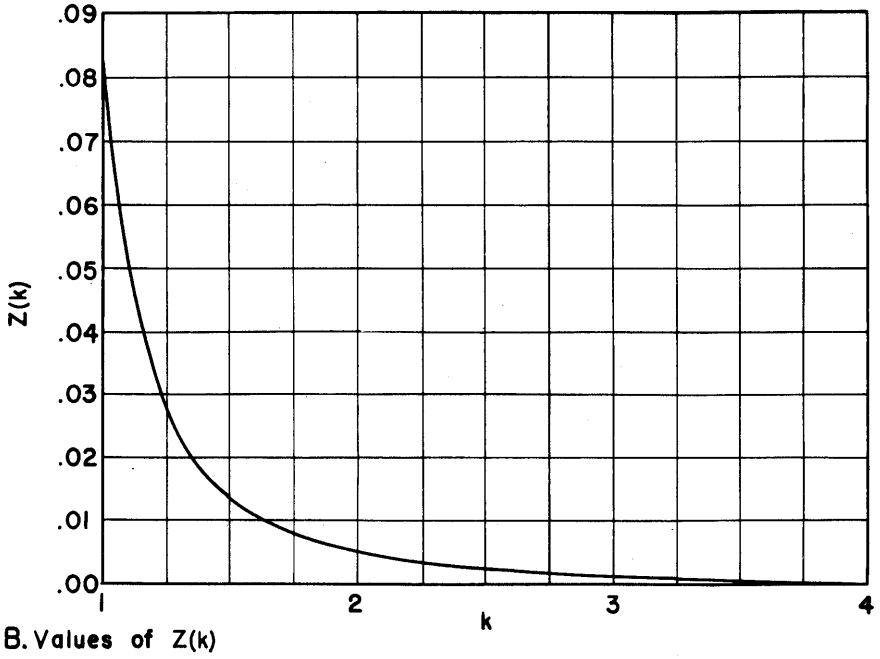

B. Values of Z(k)

Figure 5

Functions of "k", Transverse Bending

$$P = C(k)\frac{A^2}{B}bt + A'_s f'_s + A_s f_s \qquad (34)$$

Taking moments of all forces about the center line gives

$$Pe = C(k)\frac{A^2}{B}bt^2 Z(k) + \frac{(t-2d')}{2}\left(A'_s f'_s - A_s f_s\right) \qquad (35)$$

Eliminating P between Equations (34) and (35) gives

$$C(k)\frac{A^2}{B}bt\left[e - Z(k)t\right] + A'_s f'_s\left(e - \frac{t}{2} + d'\right) + A_s f_s\left(e + \frac{t}{2} - d'\right) = 0 \qquad (36)$$

If the steel areas in the two flanges are equal, this equation becomes

$$C(k)\frac{A^2}{B}\left[\frac{e}{t} - Z(k)\right] + \frac{p}{2}\left[f'_s\left(\frac{e}{t} - \frac{1}{2} + \frac{d'}{t}\right) + f_s\left(\frac{e}{t} + \frac{1}{2} - \frac{d'}{t}\right)\right] = 0 \qquad (37)$$

Examination of Figure 4 shows that

$$f'_s = \frac{A}{2B}\frac{\left[k^2 - \left(\frac{1}{2} + \frac{d'}{t}\right)k + \frac{d'}{2t}\right]}{\left(k^2 - k + \frac{1}{3}\right)}E_s \qquad (38)$$

and

$$f_s = \frac{\left(k - \frac{d}{t}\right)}{\left(k - \frac{d'}{t}\right)}f'_s \qquad (39)$$

AXIAL LOAD AND DIAGONAL BENDING OF SQUARE SECTIONS

Case I. Neutral Axis within Section

The theoretical development will be made for the case $0<k<1/2$ which can be shown to give an excellent approximation for $1/2<k<1$. Examination of Figure 6 shows that the total compression in the concrete can be expressed thus

$$C = \int_0^{kD} (AXx - BX^2x^2)(2kD - 2x)\,dx$$

Integrating and substituting limits give

$$C = \frac{AXk^3D^3}{3} - \frac{BX^2k^4D^4}{6} \qquad (40)$$

Differentiating Equation (40) with respect to X and equating to zero give

$$\frac{\partial C}{\partial X} = 0; \qquad X = \frac{A}{BkD} \qquad (41)$$

Substituting Equation (41) in Equation (40)

$$C = \frac{A^2k^2D^2}{6B} \qquad (42)$$

The distance from the neutral axis to the centroid of the stress volume is found by taking static moments about the axis thus

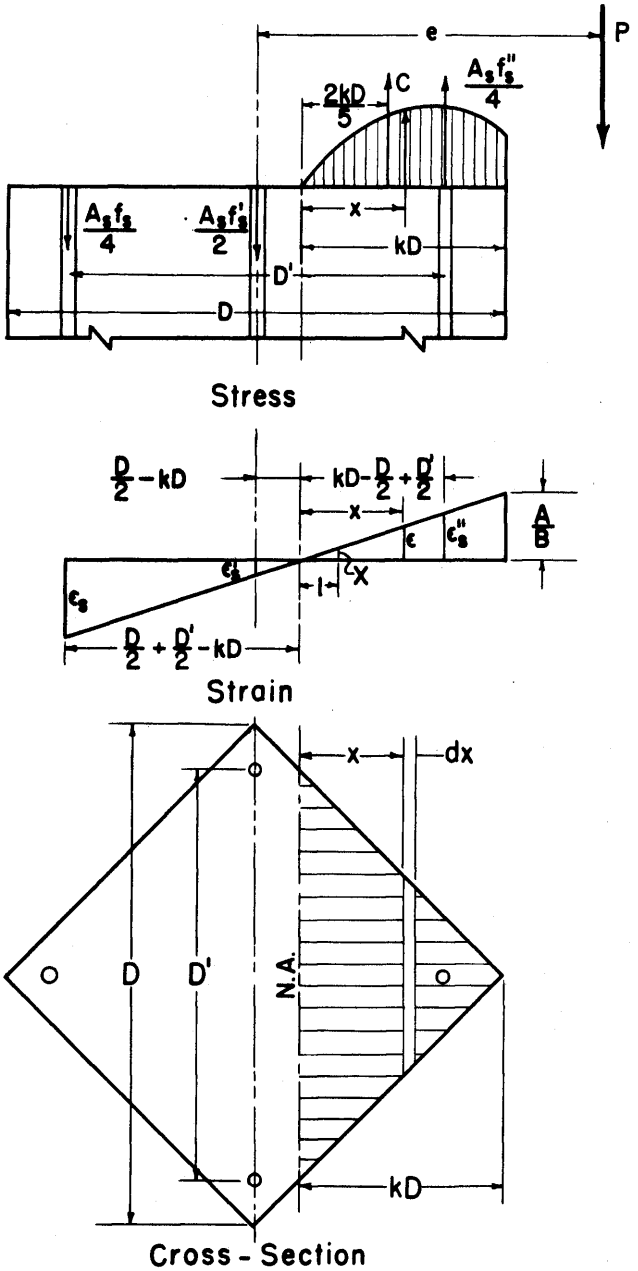

Figure 6

Axial Load and Diagonal Bending, Case I.

$$x_1 = \frac{\int f_c x\,dA}{C} = \frac{\int_0^{kD} (A\epsilon - B\epsilon^2)(D-2x)x\,dx}{\frac{A^2k^2D^2}{6B}} \qquad (43)$$

Substituting in this expression $\epsilon = Xx$, completing the integration, and substituting Equation (41) give

$$x_1 = \frac{2}{5}kD \qquad (44)$$

Projecting all forces in Figure 6 on a vertical line gives

$$P = \frac{1}{6}\frac{A^2}{B}k^2D^2 + \frac{A_s}{2}\left(\frac{f_s''}{2} - f_s' - \frac{f_s}{2}\right) \qquad (45)$$

Taking moments of all forces in Figure 6 about the center line gives

$$Pe = \frac{1}{6}\frac{A^2}{B}k^2D^2\left(\frac{D}{2} - \frac{3}{5}kD\right) + \frac{A_s}{4}\left(f_s'' + f_s\right)\frac{D'}{2} \qquad (46)$$

Eliminating P between Equations (45) and (46)

$$\frac{1}{6}\frac{A^2}{B}k^2\left(\frac{1}{2} - \frac{3}{5}k - \frac{e}{D}\right) + \frac{p}{4}\left[\frac{f_s''}{2}\left(\frac{D'}{2D} - \frac{e}{D}\right) + f_s'\left(\frac{e}{D}\right)\right.$$

$$\left. + \frac{f_s}{2}\left(\frac{D'}{2D} + \frac{e}{D}\right)\right] = 0 \qquad (47)$$

Examination of Figure 6 shows that

$$f_s'' = \frac{A}{B}\left[1 - \frac{1}{2k}\left(1 - \frac{D'}{D}\right)\right]E_s \qquad (48)$$

$$f_s' = \frac{(1-2k)}{\left(2k-1+\frac{D'}{D}\right)} f_s'' = \frac{A}{B}\left(\frac{1}{2k}-1\right)E_s \qquad (49)$$

and

$$f_s = \frac{\left(\frac{D'}{D}+1-2k\right)}{\left(\frac{D'}{D}-1+2k\right)} f_s'' \qquad (50)$$

Case II. Neutral Axis outside Section

In the case of compression over the entire section, it can be seen from Figure 7 that the total compression on the concrete will be

$$C = 2\int_{kD-D}^{kD-\frac{D}{2}} (AXx - BX^2x^2)\left[x - D(k-1)\right]dx$$

$$+ 2\int_{kD-\frac{D}{2}}^{kD} (AXx - BX^2x^2)(kD - x)dx$$

Integrating and substituting limits give

$$C = \frac{XD^3}{2}\left[A\left(k - \frac{1}{2}\right) - BXD\left(k^2 - k + \frac{7}{24}\right)\right] \qquad (51)$$

Differentiating with respect to X and placing equal to zero give

$$\frac{\partial C}{\partial X} = 0; \qquad X = \frac{A\left(k - \frac{1}{2}\right)}{2BD\left(k^2 - k + \frac{7}{24}\right)} \qquad (52)$$

Substituting Equation (52) in Equation (51)

$$C = \frac{D^2}{8}\cdot\frac{A^2}{B}\cdot\frac{k(k-1) + \frac{1}{4}}{k(k-1) + \frac{7}{24}} \qquad (53)$$

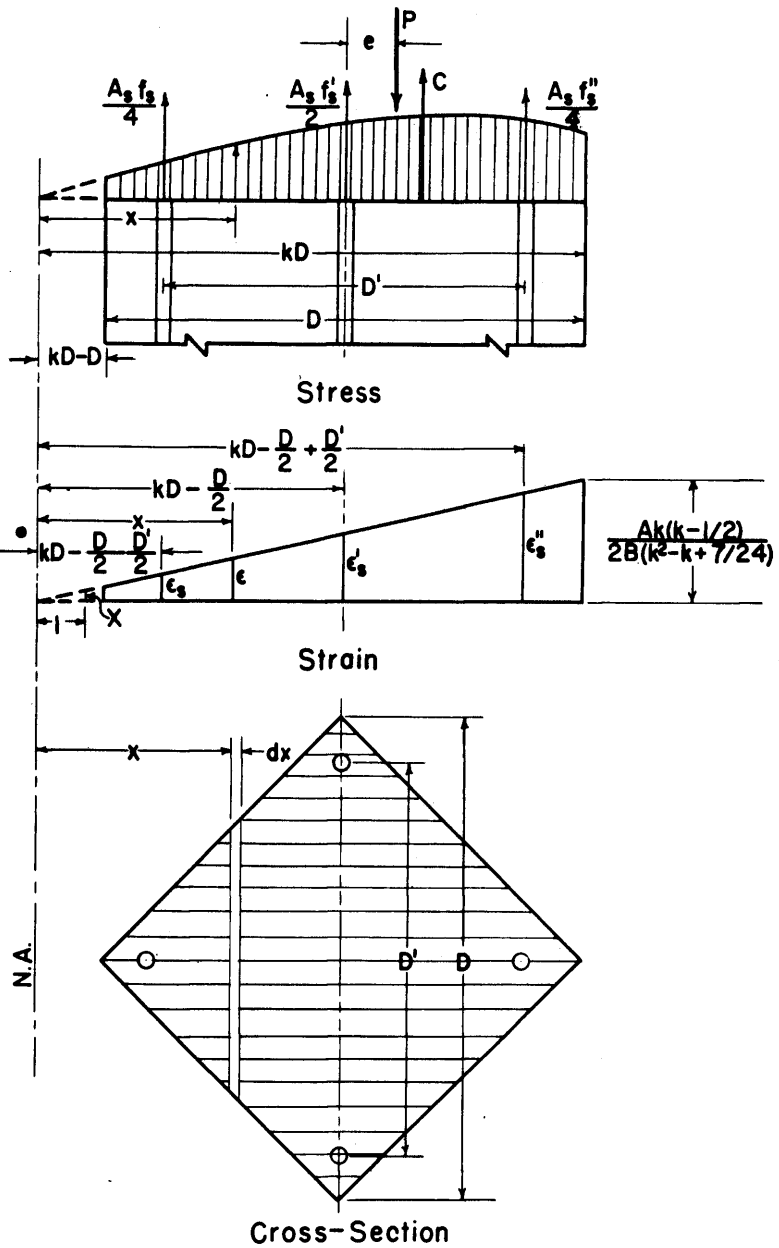

Figure 7

Axial Load and Diagonal Bending, Case II

In order to facilitate numerical computation, the variation of the function

$$\phi(k) = \frac{k(k-1)+\frac{1}{4}}{8\left[k(k-1)+\frac{7}{24}\right]} \tag{54}$$

has been plotted in Figure 8. The distance from the neutral axis to the centroid of the stress volume is found by taking statical moments about the axis, thus

$$x_1 = \frac{\int f_c x\,dA}{C} = \frac{\int_{kD-D}^{kD} (A\epsilon - B\epsilon^2) y x\,dx}{\frac{D^2A^2}{8B}\phi(k)} \tag{55}$$

Substituting in this expression $\epsilon = Xx$, completing the integration, and substituting Equation (52) give

$$x_1 = \frac{k^4-2k^3+\frac{37}{24}k^2-\frac{13}{24}k+\frac{11}{144}}{\left(k-\frac{1}{2}\right)\left(k^2-k+\frac{7}{24}\right)} D \tag{56}$$

The distance from the center of section to the centroid of stress volume can be seen from Figure 7 to equal

$$x_1' = \left[\frac{k^4-2k^3+\frac{37}{24}k^2-\frac{13}{24}k+\frac{11}{144}}{\left(k-\frac{1}{2}\right)\left(k^2-k+\frac{7}{24}\right)} - k + \frac{1}{2}\right] \cdot D \tag{57}$$

Again to facilitate numerical computation, the variation of the function

$$\psi(k) = \frac{k^4-2k^3+\frac{37}{24}k^2-\frac{13}{24}k+\frac{11}{144}}{\left(k-\frac{1}{2}\right)\left(k^2-k+\frac{7}{24}\right)} - k + \frac{1}{2} \tag{58}$$

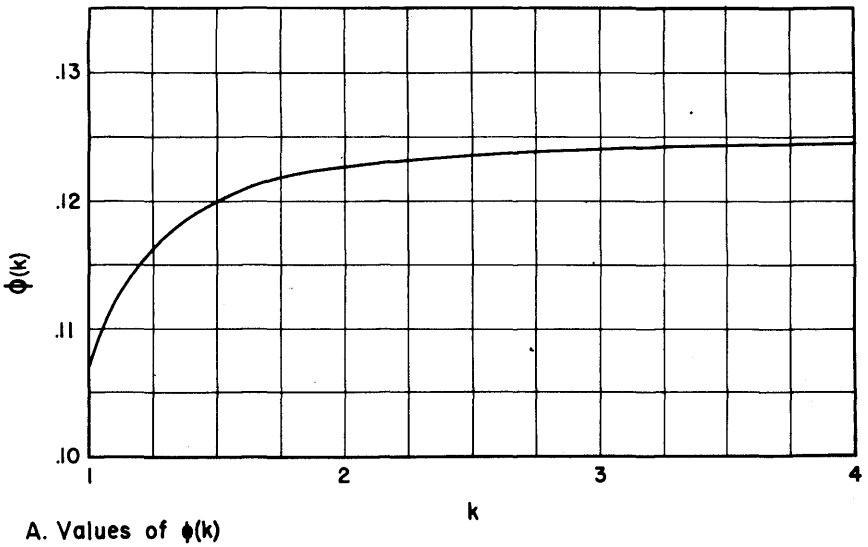

A. Values of $\phi(k)$

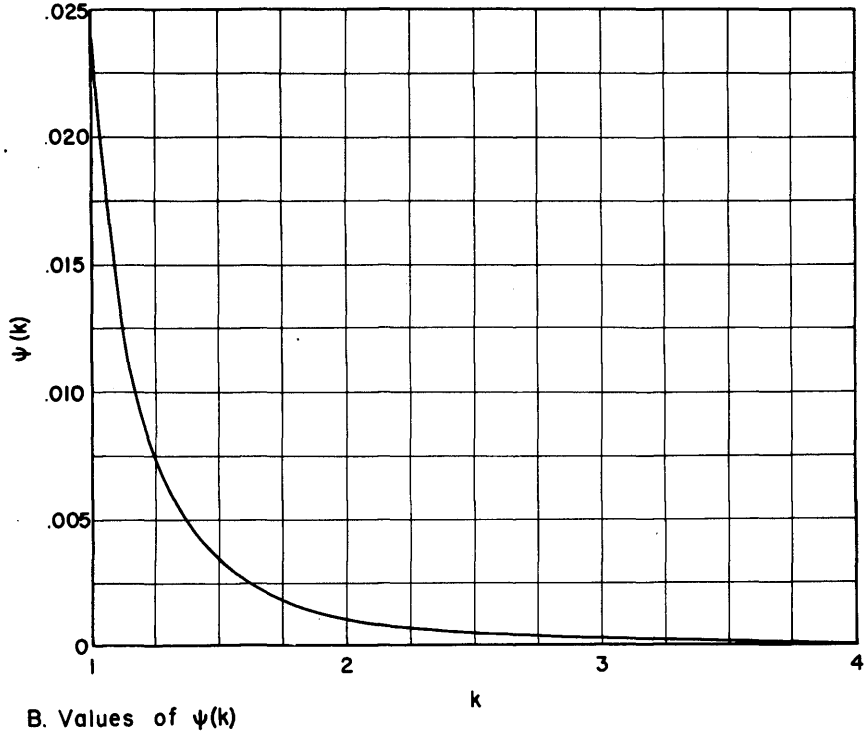

B. Values of $\psi(k)$

Figure 8

Functions of "k", Diagonal Bending

has been plotted in Figure 8.

Projecting all forces in Figure 7 on a vertical line gives

$$P = \frac{A^2}{B} D^2 \phi(k) + A_s \left(\frac{f_s}{4} + \frac{f_s'}{2} + \frac{f_s''}{4} \right) \tag{59}$$

Taking moments of all forces about the center line gives

$$Pe = \frac{A^2}{B} D^3 \phi(k) \cdot \psi(k) + \frac{A_s}{4} \left(f_s'' - f_s \right) \left(\frac{D}{2} - d' \right) \tag{60}$$

Eliminating P between Equations (59) and (60)

$$\frac{A^2}{B} \phi(k) \left[\frac{e}{D} - \psi(k) \right] + \frac{p}{4} \left[\frac{f_s''}{2} \left(\frac{D'}{2D} - \frac{e}{D} \right) - f_s' \left(\frac{e}{D} \right) - \frac{f_s}{2} \left(\frac{D'}{2D} + \frac{e}{D} \right) \right] = 0 \tag{61}$$

Examination of Figure 7 shows that

$$f_s'' = \frac{A}{2B} \frac{\left(k - \frac{1}{2} + \frac{D'}{2D} \right) \left(k - \frac{1}{2} \right)}{\left(k^2 - k + \frac{7}{24} \right)} E_s \tag{62}$$

$$f_s' = \frac{\left(k - \frac{1}{2} \right)}{\left(k - \frac{1}{2} + \frac{D'}{2D} \right)} f_s'' \tag{63}$$

and

$$f_s = \frac{\left(k - \frac{1}{2} - \frac{D'}{2D} \right)}{\left(k - \frac{1}{2} + \frac{D'}{2D} \right)} f_s'' \tag{64}$$

APPROXIMATE COLUMN DEFLECTION

The structural arrangement for transmission of the eccentric load to the columns was such that considerable rotations occurred at the ends. These, in turn, caused large horizontal deflections which influenced the final stresses in the specimens. A method of evaluating these deflections is given below.

Figure 9 shows the column, hinged at both ends and eccentrically loaded with an ultimate load of P, which produces a deflection, δ, at mid-height. This horizontal deflection consists of two parts as shown.

$$\delta = \delta_1 + \delta_2$$

If a circular arc is substituted for EG, it is seen that

$$\frac{1}{\rho} = \frac{\epsilon}{kt} \tag{65}$$

where ρ is the radius of curvature, ϵ, the unit strain at the extreme fibers and kt is the distance to the neutral axis. From the right triangle OEF it is seen that

$$\frac{1}{\rho} = \frac{8\delta_1}{l_1^2 + 4\delta_1^2} \tag{66}$$

Since the second term of the denominator is extremely small compared to the first term, it follows that

$$\frac{1}{\rho} = \frac{8\delta_1}{l_1^2} \tag{67}$$

Eliminating the radius of curvature between Equations (65) and (67) gives

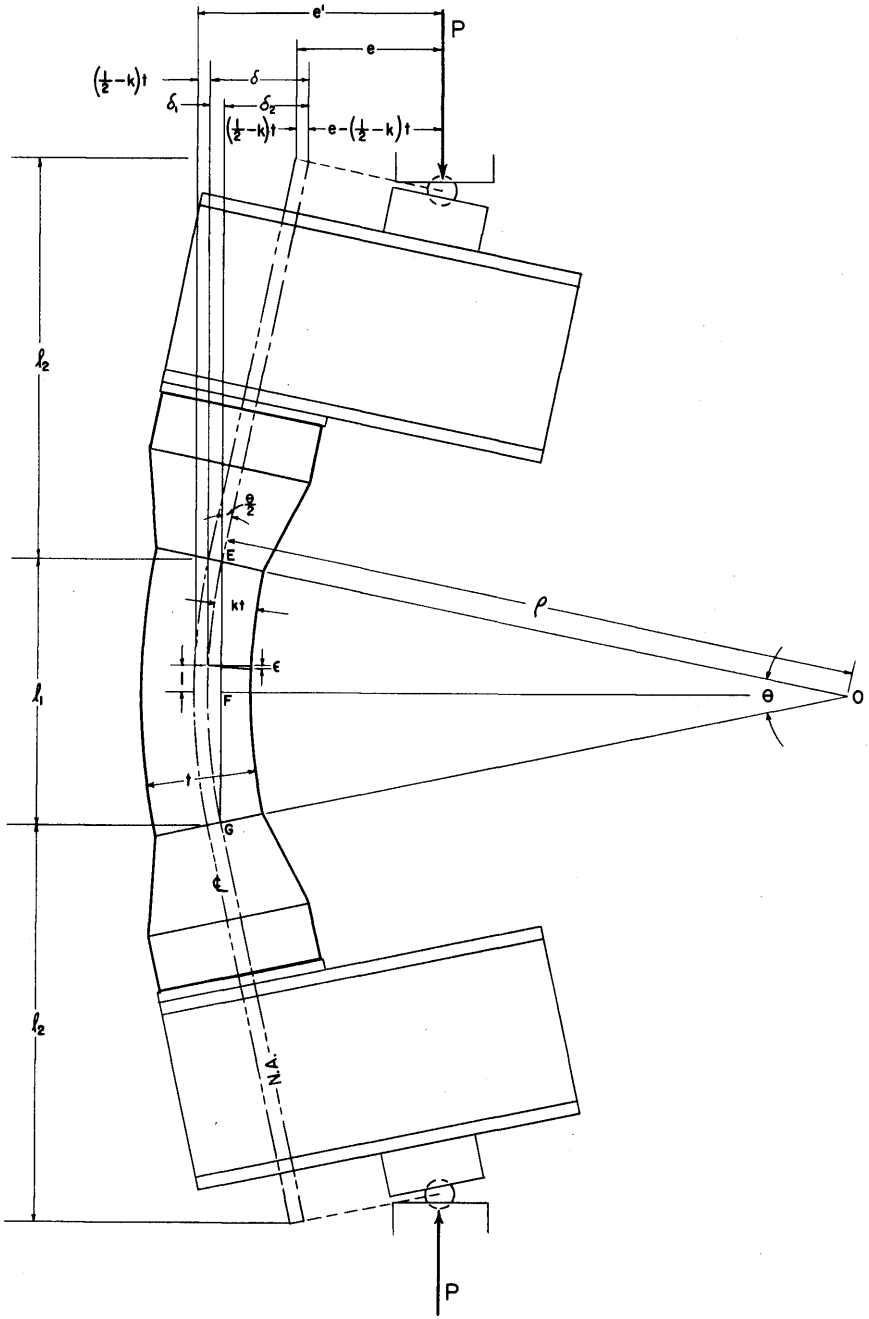

Figure 9

Evaluation of Deflection

$$\delta_1 = \frac{l_1^2 \epsilon}{8kt} \tag{68}$$

The enlarged ends and steel brackets have considerable rigidity compared to the central portion. The ends may therefore be assumed to be tangents to the circular arc of the central portion. From Figure 9 it is seen that

$$\delta_2 = l_2 \frac{\theta}{2} \tag{69}$$

and

$$\theta = \frac{l_1}{\rho} \tag{70}$$

Substituting Equation (67) in Equation (70)

$$\theta = \frac{8\delta_1}{l_1} \tag{71}$$

The total deflection will equal

$$\delta = \delta_1 + \delta_2 = \delta_1 + \frac{4\delta_1}{l_1} l_2 = \delta_1 \left(1 + 4\frac{l_2}{l_1}\right) \tag{72}$$

Substituting Equation (68)

$$\delta = \frac{l_1(l_1 + 4l_2)}{8kt} \epsilon \tag{73}$$

For the square section subjected to combined axial load and transverse bending, the extreme fiber unit strain is equal to 3A ÷ 4B (see Equation 19), while for combined axial load and diagonal bending this quantity equals A ÷ B (see Equation 41). The deflections can therefore be written

$$\delta = \frac{l_1(l_1 + 4l_2)}{8kt} \frac{3A}{4B} \tag{74}$$

for the square section subjected to axial load and transverse bending and

$$\delta = \frac{l_1(l_1 + 4l_2)}{8kD} \frac{A}{B} \tag{75}$$

for the square section subjected to axial load and diagonal bending.

TEST SPECIMENS

The tests were made with ten specimens of dimensions shown in Figure 10 and reinforced with four round steel bars of different sizes as indicated in Table I. In addition to the longitudinal reinforcement, there were in each specimen eight lateral ties of 1/8 inch diameter.

The Portland cement used in manufacturing the concrete passed the standard specifications of the American Society for Testing Materials. Owing to the small clearance between reinforcement and forms, pea gravel, passing a 3/8 inch sieve and retained by a No. 4 sieve, was used for coarse aggregate. The fine aggregate was sand with a fineness modulus of 2.96 and a surface modulus of 16.96. The water-cement ratio of the concrete was 5.65 gallons per sack, and the average slump was 2.3 inches.

A total of ten 6-inch by 12-inch standard control cylinders was tested. The cylinder strength, f'_c, varied from 4740 pounds per square inch to 5950 pounds per square inch with an average value of 5435 pounds per square inch. The stress-strain curves were obtained by placing a concrete inside, but not in contact with, a concentrical steel cylinder of slightly greater diameter. The concrete and steel cylinders were of the same height, and both were equipped with electrical strain gages for measuring their deformations in the axial direction. The steel cylinder was first calibrated so that the amount of load it was carrying could be determined from the deformation measurements. The total load and the load carried by the steel were recorded, and the load on the concrete cylinder equated to the difference. From these observations, the stress-strain curves for the concrete were drawn. Figure 11 shows the arrangement of testing and Figure 12 the appearance of two typical cylinders after compression tests to failure. The average stress-strain curve in Figure 1 gave values of Coefficients $A = 5435 \times 10^3$ and $B = 1359 \times 10^6$.

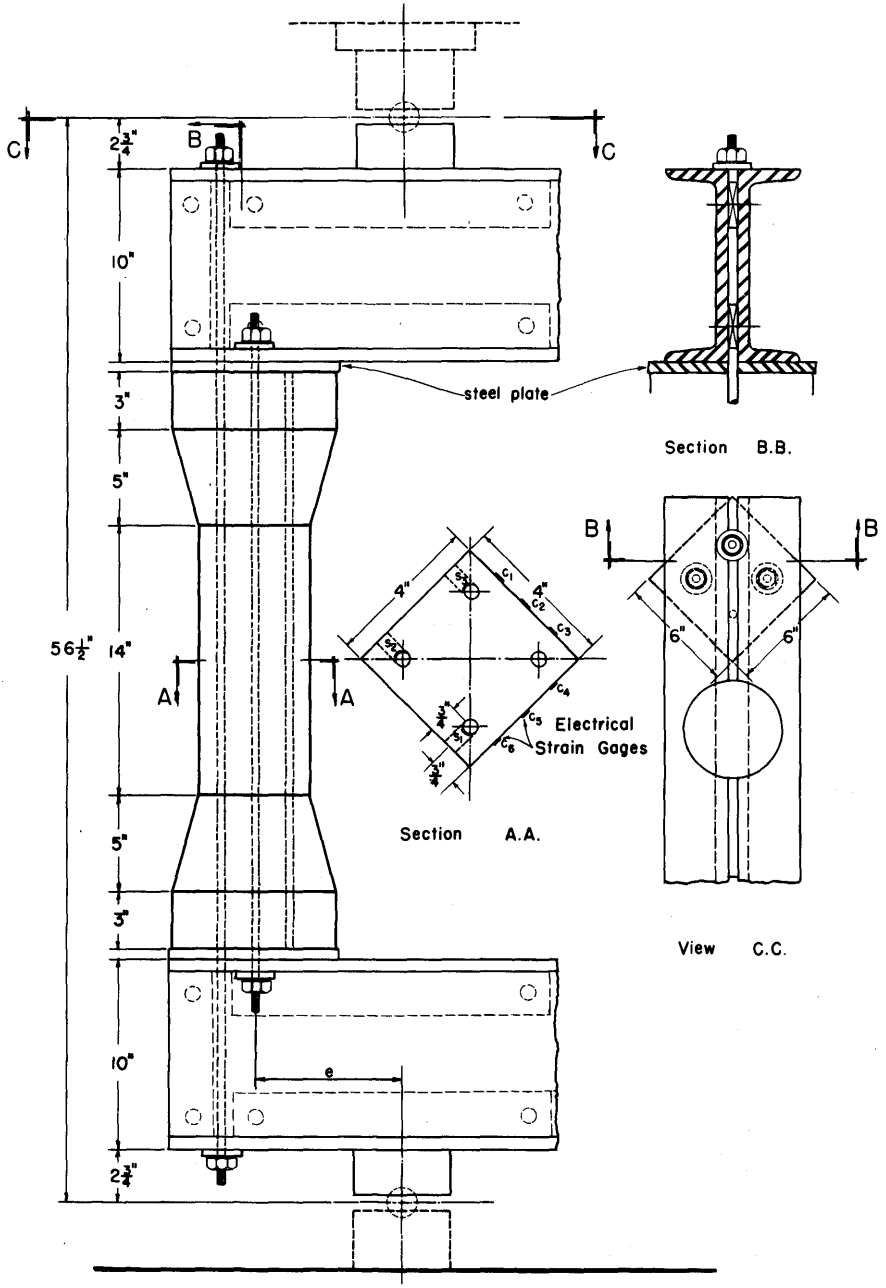

Figure 10

Test Specimen

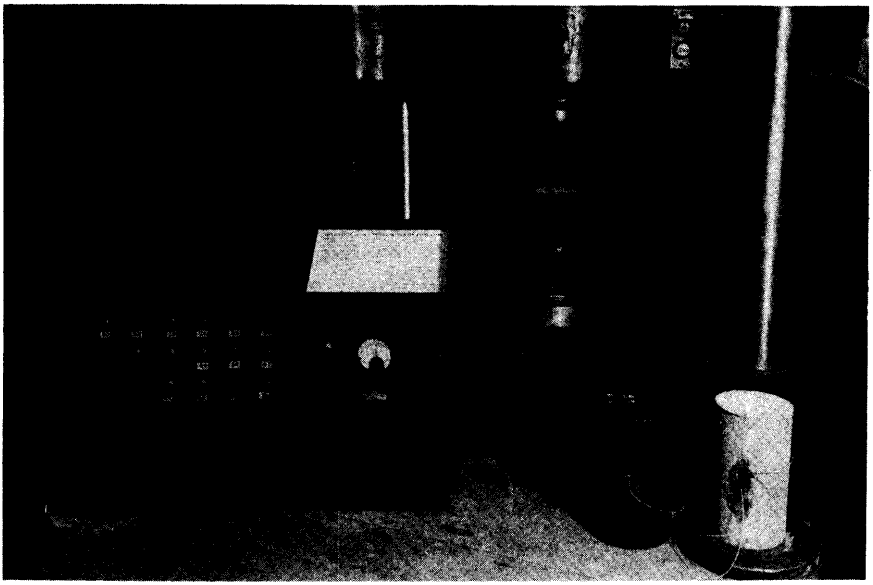

Figure 11. Arrangement of Special Cylinder Test

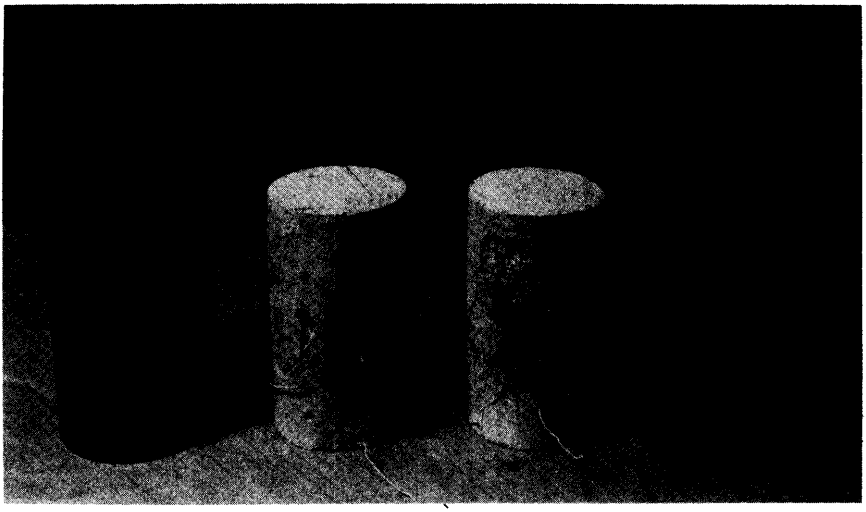

Figure 12. Typical Cylinder Failures

The steel reinforcing bars were subjected to the usual standard tensile tests in duplicate. The average values of the yield point and modulus of elasticity for each type of bar are listed in Table I.

The ten column specimens were tested in duplicate with a constant 4-inch eccentricity on the line of a diagonal. Structural steel brackets (see Figure 10) were used for application of the eccentric load to the specimen. The longitudinal reinforcing bars in the compression portion of the section were milled to the exact lengths to insure direct bearing against the steel brackets, while the tension bars were projected through the steel brackets.

Nine electrical strain gages (gage factor 2.04 $\pm$ 1 per cent, resistance 120.0 $\pm$ 0.2 ohms) were attached to each specimen. Six of these were on the surface of the compression side of the concrete and three were on the surface of the tensile steel in small slots as shown in Figure 10. In order to prevent weakening of the column by reduction of section, the small slots for the steel gages were placed at three different levels.

The tests were carried out by applying the load through the ball bearings at both the top and the bottom of the specimen as shown in Figure 13. The arrangement of equipment is shown in Figure 14.

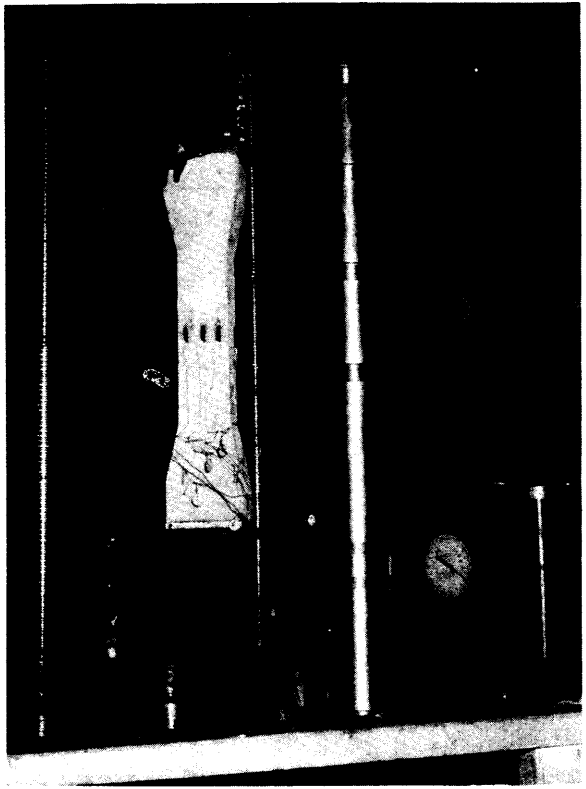

Figure 13. Arrangement of Eccentrically Loaded Column Test

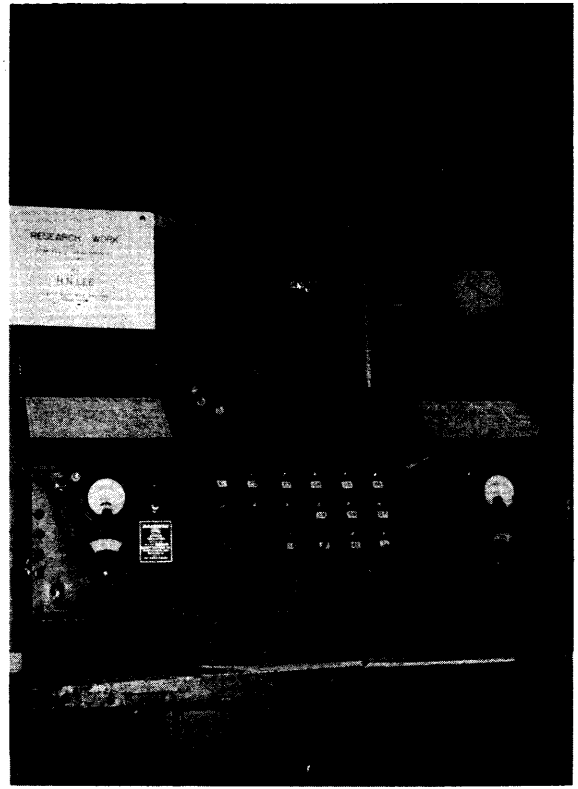

Figure 14. Arrangement of Equipment

TABLE I

Test Results

Specimen	Steel	E_s 10^6psi	f_y ksi	p	Actual Ultimate P #	Ave.	Ave. Actual k	δ From Equation 75	$\frac{e+\delta}{D}$	k From Equation 47	Computed P #
SC1 SC6	4-1/4"ϕ	30	35.8	.0123	5270 4675	4972	.281	.435	.7840	.273	5102
SC2 SC7	4-5/16"ϕ	30	39.2	.0192	7440 7250	7345	.366	.334	.7661	.345	7768
SC3 SC8	4-3/8"ϕ	30	40.2	.0276	9500 9810	9655	.398	.308	.7615	.388	9774
SC4 SC9	4-1/2"ϕ	29	45.6	.0491	13500 14300	13900	.441	.278	.7562	.431	14209
SC5 SC10	4-5/8"ϕ	29	40.7	.0766	16475 16500	16488	.454	.270	.7548	.457	17483

Note: Average f'_c = 5435; Average ϵ' = .002; e = 4 inches;
$D' \div D = .625$; $A^2 \div B = 2.17 \times 10^4$; $A \div B = 4 \times 10^{-3}$.

TEST RESULTS

The specimens were tested to destruction by increasing the load by increments of 500 pounds. Strain gage readings were recorded for each increment. Plots of these strains confirmed the assumption of the preservation of plane sections and established for each loading the position of the neutral axis. The ultimate positions of this line are listed in Table I. The table also lists ultimate loads actually recorded and corresponding values computed by the formulas derived in this bulletin. The steps in computation of the values in Table I for the specimens SC2 and SC7 are presented to outline the procedure. Preliminary tests showed that $A^2 \div B = 2.17 \times 10^4$, $A \div B = 4 \times 10^{-3}$, $f_y = 39200$ pounds per square inch, and $E_s = 30 \times 10^6$ pounds per square inch. The ultimate position of the neutral axis during the test as indicated by strain gages was $k = .366$. Substituting these values and the dimensions of the test specimen (Figure 10) in Equation (75) gives

$$\delta = \frac{14(14 + 4 \times 21.25)}{8 \times .366 \times 5.66} \times 4 \times 10^{-3} = .334$$

then

$$\frac{e + \delta}{D} = \frac{4 + .334}{5.66} = .7661$$

The yield point of the reinforcing steel is $f_y = 39200$ pounds per square inch. It can be shown by Equations (48), (49), and (50) for $.281 < k < .375$ that

$$f_s = f_s' = f_s'' = 39200 \text{ p.s.i.}$$

Equation (47) then becomes

$$k^2(.2661 + .6k) = .056114$$

Solution by trial gives k = .345. When all the reinforcing steel is stressed to the yield point, Equation (45) reduces to

$$P = \frac{1}{6}\frac{A^2}{B}k^2D^2 - \frac{D^2}{4}pf_y$$

Substituting all the known values in this equation gives

$$P = 13789 - 6021 = 7768\#$$

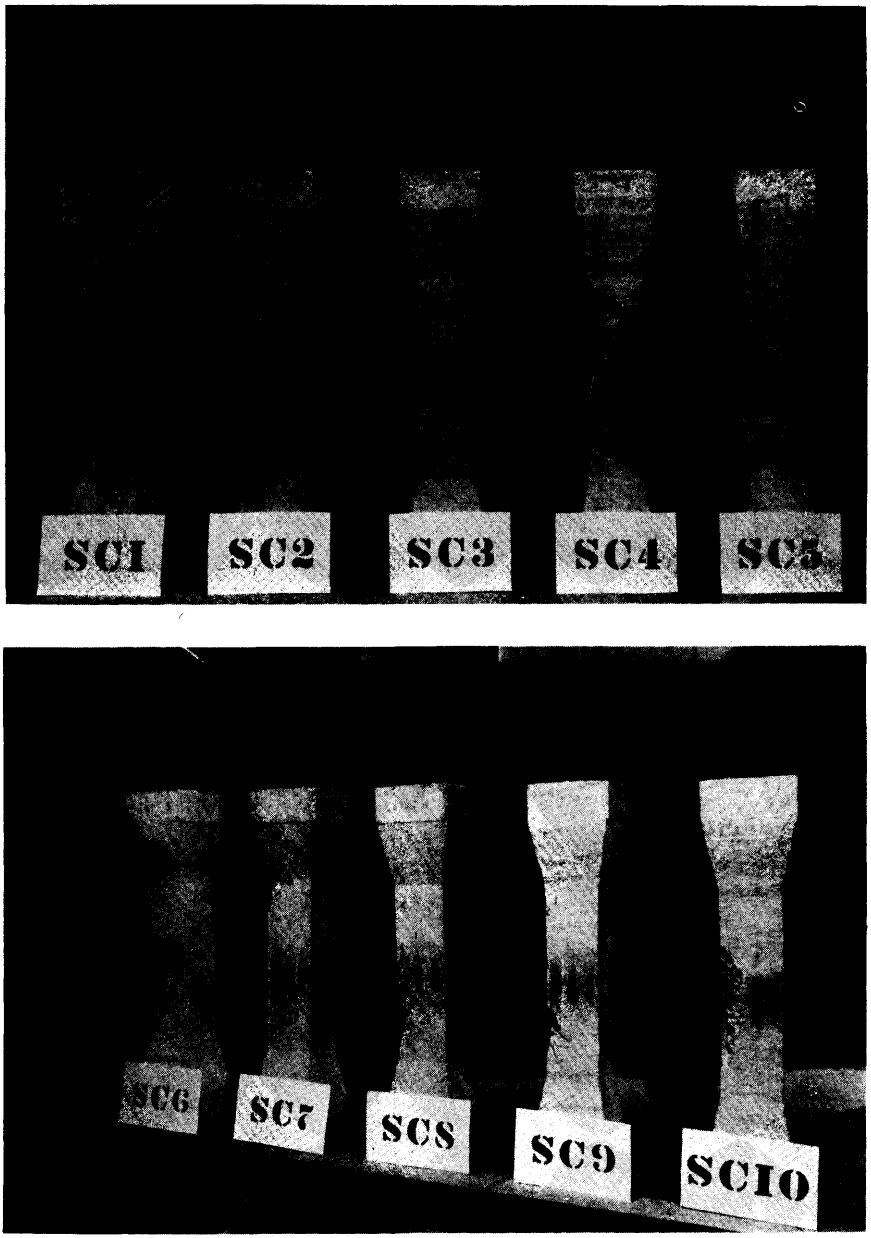

Figure 15. Appearances of Column Failures

CONCLUSIONS

Appearances of column failures are shown in Figure 15. Crushing of the concrete (usually near the center portion) due to excessive compression was accompanied by opposite tension cracks caused by yield point stresses in the reinforcement.

From the data presented in Table I, it is believed that the following conclusions can be drawn:

1. The modified plastic theory gives results, for position of neutral axis and ultimate load, which are in accordance with actual test results.

2. The ultimate supporting capacity of eccentrically loaded sections increases with the steel percentage.

3. The ultimate supporting capacity of a column subjected to an eccentric load will be influenced by the horizontal deflection of the column.

The Engineering Experiment Station of the University of Minnesota was established by an act of the Board of Regents on December 13, 1921.

The purpose of the Station is to advance research and graduate study in the Institute of Technology, to conduct scientific and industrial investigations, and to cooperate with governmental bodies, technical societies, associations, industries, or public utilities in the solution of technical problems. The results of scientific investigations will be published in the form of bulletins and technical papers. Information which is of general interest and yet not the result of original research may be distributed in the form of circulars.

For a complete list of publications or other information concerning the work of the Station, address the Director of the Engineering Experiment Station.

BULLETINS AVAILABLE

12. Thermal Conductivity of Building Materials, by F. B. Rowley and A. B. Algren. x + 134 pages, 109 illustrations. 1937. $1.50. (Purchased through University Press.)
14. Square Sections of Reinforced Concrete under Thrust and Nonsymmetrical Bending, by Paul Andersen. vi + 42 pages, 8 figures, 23 diagrams. 1939.
15. Laboratory Studies of Asphalt Cements, by F. C. Lang and T. W. Thomas. x + 96 pages, 43 illustrations. 1939.
16. Factors Affecting the Performance and Rating of Air Filters, by F. B. Rowley and R. C. Jordan. viii + 54 pages, 21 illustrations. 1939.
18. Condensation of Moisture and Its Relation to Building Construction and Operation, by F. B. Rowley, A. B. Algren, and C. E. Lund. vi + 69 pages, 28 illustrations. 1941.
19. Pulp, Paper, and Insulation Mill Waste Analysis, by F. B. Rowley, R. C. Jordan, R. M. Olson, and R. F. Huettl. vi + 55 pages, 34 illustrations. 1942.
20. Conservation of Fuel, by F. B. Rowley, R. C. Jordan, and C. E. Lund. vi + 61 pages, 22 illustrations, 17 tables. 1943.

21. Aids to Technical Writing, by R. C. Jordan and M. J. Edwards. viii + 112 pages, 60 illustrations, 13 tables. May, 1944.
22. Vapor Transmission Analysis of Structural Insulating Board, by F. B. Rowley and C. E. Lund. vi + 71 pages, 24 illustrations, 16 tables. October, 1944.
24. Factors Affecting Heat Transmission through Insulated Walls, by F. B. Rowley and C. E. Lund. iv + 25 pages, 8 illustrations, 8 tables. April, 1946.
25. Vapor Resistant Coatings for Structural Insulating Board, by F. B. Rowley, M. H. LaJoy and E. T. Erickson. vi + 31 pages, 9 illustrations, 10 tables. September, 1946.
26. Moisture and Temperature Control in Buildings Utilizing Structural Insulating Board, by F. B. Rowley, M. H. LaJoy, and E. T. Erickson. vi + 38 pages, 16 illustrations, 8 tables. July, 1947.
27. Water Permeability of Structural Clay Tile Facing Walls, by J. A. Wise. iv + 32 pages, 26 illustrations, 4 tables. August, 1948.
28. Thermal Properties of Soils, by M. S. Kersten. xiv + 227 pages, 138 illustrations, 15 tables, 5 plates. June, 1949.
29. Proceedings of the Symposium on Engineering Research, edited by C. E. Lund. x + 110 pages. August, 1949.
30. Some Causes of Paint Peeling, by F. B. Rowley and M. H. LaJoy. vi + 34 pages, 23 illustrations, 11 tables. September, 1949.
31. Determination of Load Distribution on a Beam from Measurements on Its Deflected Form, by P. Andersen and S. Mukhopadhyay. x + 56 pages, 16 illustrations, 13 tables. January, 1950.
32. Determination of Particle Size Distribution--Apparatus and Technique for Flour Mill Dust, by K. T. Whitby. viii + 39 pages, 27 illustrations, 1 table. January, 1950.

TECHNICAL PAPERS AVAILABLE

1. Condensation within Walls, by F. B. Rowley, A. B. Algren, and C. E. Lund. 12 pages. January, 1938.
32. Construction and Operation of a 15-Inch Cupola, by F. Holtby. 4 pages. August, 1941.
42. Abnormal Currents in Distribution Transformers Due to Lightning, by J. M. Bryant and M. Newman. 5 pages. September, 1942.
46. Discoloration Method of Rating Air Filter, by F. B. Rowley and R. C. Jordan. 10 pages. September, 1943.
48. Valve Guide Leakage in an Automotive Engine, by M. A. Lindeman and B. J. Robertson. 22 pages. May, 1944.
52. Carbon Dioxide Variation in a Vented Stack, by M. H. LaJoy. 27 pages. May, 1945.
53. Thermal Conductivity of Insulating Material at Low Mean Temperatures, by F. B. Rowley, R. C. Jordan, and R. M. Lander. 6 pages. December, 1945.
56. Calculation of Bearing Capacities of Footings by Circular Arcs, by Paul Andersen, 3 pages. June, 1946.
60. Comfort Reactions of 275 Workmen during Occupancy of Air-Conditioned Offices, by F. B. Rowley, R. C. Jordan, and W. E. Snyder. 4 pages. June, 1947.
62. A Statistical Analysis of Water Works Data for 1945, by G. J. Schroepfer, A. S. Johnson, H. F. Seidel, and M. B. Al-Hakim. 32 pages. October, 1948.
63. Theory and Use of Capillary Tube Expansion Device, by M. M. Bolstad and R. C. Jordan. 6 pages. December, 1948.
65. Impact Strength Testing Machine, by F. B. Rowley and M. H. LaJoy. 16 pages. June, 1949.
66. Ground Temperatures as Affected by Weather Conditions, by A. B. Algren. 6 pages. June, 1949.
67. Theory and Use of Capillary Tube Expansion Device, Part II, Nonadiabatic Flow, by M. M. Bolstad and R. C. Jordan. 7 pages. June, 1949.
68. Thermal Conductivity of Soils, by M. S. Kersten. 19 pages. July, 1949.
69. Specific Heat Tests on Soils, by M. S. Kersten. 5 pages. May, 1949.

71. Continuous Flow Stirred-Tank Reactor Systems. I. Design Equations for Homogeneous Liquid Phase Reactions, by J. W. Eldridge and E. L. Piret. 10 pages. June, 1950.
72. Resistance Gradients through Viscous Coated Air Filters, by F. B. Rowley and R. C. Jordan. 8 pages. December, 1949.
73. Crushing of Single Particles of Crystalline Quartz, by J. W. Axelson and E. L. Piret. 6 pages. April, 1950.
74. Continuous Flow Stirred Tank Reactor Systems. Development of Transient Equations, by D. R. Mason and E. L. Piret. 9 pages. May, 1950.
75. Hot Wire Anemometry, by G. B. Middlebrook and E. L. Piret. 3 pages. August, 1950.
76. Snow, Ice, and Permafrost, by R. C. Jordan, and H. T. Mantis. 5 pages. October, 1950.
77. Bathymetric Chart of Lake Michigan, by K. O. Emery. 16 pages. April, 1951.
78. Effect of Continuously Controlled pH on Lactic Acid Fermentation, by L. L. Kempe, H. O. Halvorson, and E. L. Piret. 6 pages. September, 1950.
79. Lactic Acid Fermentation Rate, by R. K. Finn, H. O. Halvorson, and E. L. Piret. 5 pages. September, 1950.

CIRCULARS AVAILABLE

2. Wartime Refrigeration Training at the University of Minnesota, by R. C. Jordan and C. E. Lund. 3 pages. September, 1944.
3. Five-Year Mechanical Engineering Curriculum, by R. C. Jordan. 5 pages. January, 1947.
4. The Transport of Solid Particles in a Fluid Stream--A Bibliography with Abstracts, by W. B. Hendry. 28 pages. October, 1949.